Flat layered structure and improved photoluminescence emission from porous silicon microcavities formed by pulsed anodic etching

Z.H. Xiong[1,*]**, L.S. Liao**[1]**, X.M. Ding**[1]**, S.H. Xu**[1]**, Y. Liu**[1]**, L.L. Gu**[1]**, F.G. Tao**[2]**, S.T. Lee**[3]**, X.Y. Hou**[1]

[1] Surface Physics Laboratory, Fudan University, Shanghai 200433, P.R. China
[2] Department of Chemistry, Fudan University, Shanghai 200433, P.R. China
[3] Department of Physics and Materials Science, City University of Hong Kong, P.R. China

Abstract. Single-mode, highly directional and stable photoluminescence (PL) emission has been achieved from porous silicon microcavities (PSMs) fabricated by pulsed electrochemical etching. The full width at half maximum (FWHM) of the narrow PL peak available from a freshly etched PSM is about 9 nm. The emission concentrates in a cone of $10°$ around the normal of the sample, with a further reduced FWHM of ~ 5.6 nm under angle-resolved measurements. Only the resonant peak is present in such angle-resolved PL spectra. No peak broadening is found upon exposure of the freshly prepared PSM to a He−Cd laser beam, and the peak becomes somewhat narrower (~ 5.4 nm) after the PSM has been stored in an ambient environment for two weeks. At optimized etching parameters, even a 4-nm FWHM is achievable for the freshly etched PSM. In addition, scanning electron microscopy (SEM) plane-view images reveal that the single layer porous Si formed by pulsed current etching is more uniform and flatter than that formed by direct current (dc) etching, demonstrated by the well-distributed circular pores with small size in the former in comparison with the irregular interlinking pores in the latter. The SEM cross-section images show the existence of oriented Si columns of 10 nm diameter along the etching direction within the active layer, good reproducibility and flat interfaces. It is thus concluded that pulsed current etching is superior to dc etching in obtaining flat interfaces within the distributed Bragg reflectors because of its minor lateral etching.

PACS: 82.40.Mw; 78.55.Mb; 61.16.Bg

The discovery of strong visible light emission from porous silicon (PSi) at room temperature [1] has opened a new era for seeking Si-based optoelectronic devices. However, the photoluminescence (PL) or electroluminescence (EL) peaks observed from single layer PSi films are all broadened bands with large emission angles. By employing microcavity techniques [2–6], the wide-band, large-angle emission can be

narrowed, directed, and tuned in porous silicon microcavities (PSMs). It is well known that highly directional light emission will benefit the coupling efficiency between the source and the transmission line by reducing optical power along unwanted lateral directions. Moreover, spectral sharpening of the emission with a narrow band will benefit color purification and hence optimize the transmission bandwidth. Therefore, PSMs are promising for applications in data communication and light interconnection in all Si-based optoelectronic integrated circuits. In the literature, a lobed angular distribution ($30°$ around the normal axis) has previously been reported [2, 6] for the output emission of PL and EL. However, sideband emission exists in the PL spectra of the aforementioned PSMs, as measured in tilted or normal mode. Recent studies in this lab [7–9] have shown that, superior to ordinary direct current (dc) etching, pulsed current etching can yield uniform PSi films, which are obviously important for a PSM having many interfaces. We therefore consider it a possible method for improving the interface geometry, and hence the optical properties as well, of the PSM. In this work, we report for the first time the fabrication of PSMs by employing a pulsed current etching technique. A flat layered structure and spatially condensed ($10°$ around the normal axis) single-mode PL emission are successfully achieved.

1 Fabrication of PSMs by pulsed anodic etching

Figure 1 is a schematic diagram of the experimental set-up for fabricating the PSMs by pulsed anodic etching. A personal computer was used to control a pulse generator via a GPIB card to produce a sequence of pulses with specific voltage and duration. The voltage output from the pulse generator was converted to a sequence of related current pulses by an amplifier. During etching, the current pulses through the etching cell were monitored by measuring the voltage drop across a resistor connected in series with the power amplifier and the etching cell.

Structurally, a PSM is composed of an active PSi layer sandwiched between two distributed Bragg-reflectors (DBRs), made up of a sequence of PSi layers with different thick-

*Corresponding author.
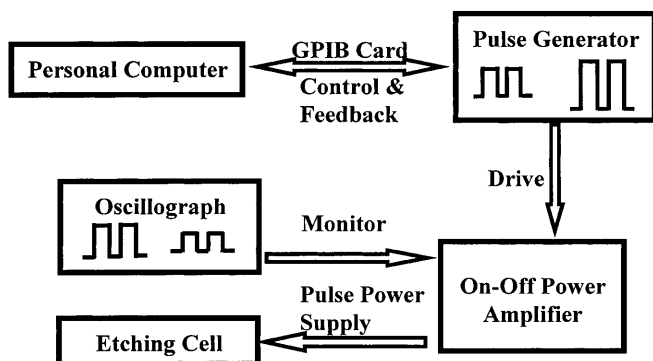(Fax: +86-21/6510-4949, E-mail: zhxiong@fudan.edu)

Fig. 1. Schematic diagram of the experimental set-up for fabricating PSMs by pulsed anodic etching

nesses and refractive indices. All the PSi layers were produced by changing current density and etching time, using the above-mentioned experimental setup, during the electrochemical etching of (100)-oriented P^+-type Si wafers (resistivity 0.01 Ωcm) in a HF solution (49%HF : C_2H_5OH : H_2O = 1 : 1 : 2). The central active PSi layer was formed by applying a current density of 83 mA/cm^2 for 7.36 s, giving rise to a refractive index n_{AC} of 1.23 and a thickness d_{AC} of 622.7 nm. These were equivalent to an optical path thickness of 766 nm, the selected wavelength λ of the cavity resonant mode [3, 10, 11]. The two DBRs were so designed that each of them was composed of a stack of 9 pairs of alternating high and low refractive index layers with their optical path thickness uniformly set at λ/4. This was accomplished by periodically applying the current density of 6.7 mA/cm^2 for 9.32 s (n_H = 2.18 and d_H = 87.9 nm) and 50 mA/cm^2 for 2.06 s (n_L = 1.42 and d_L = 134.9 nm). In all cases, the duty cycle of these pulses was 9 ms : 10 ms. This value was chosen simply because we observed considerably improved characteristics by using such a parameter. No effort was made to systematically investigate the effect of the duty cycle on the PSi structure and optical properties obtained in the present work. The anodization was performed in darkness at room temperature. Once the electrolysis process was completed, the PSM samples were immediately rinsed with de-ionized water and dried with nitrogen gas.

2 SEM micrograph

2.1 Plane-view of single layer PSi films

Images (a) and (b) in Fig. 2 are the SEM plane-view micrographs of single layer PSi fabricated by anodic dc and pulsed current etching respectively. The SEM images were taken with a Philips XL30-FEG, operated at acceleration voltages ranging from 5 to 20 kV. The etching parameters adopted were those used to form the low refractive layers in the DBRs, with the equivalent etching time kept the same in the two cases. The two images were obtained under the same measurement parameters. Due to its minor contribution to the detected emission of the secondary electron, a pore at the sample surface emerges as a dark dot in the SEM image of a PSi film, while the Si skeleton left appears as the bright part. The pore dimension ranges from several nanometers to tens of nanometers. The surface of the pulsed-current-etched
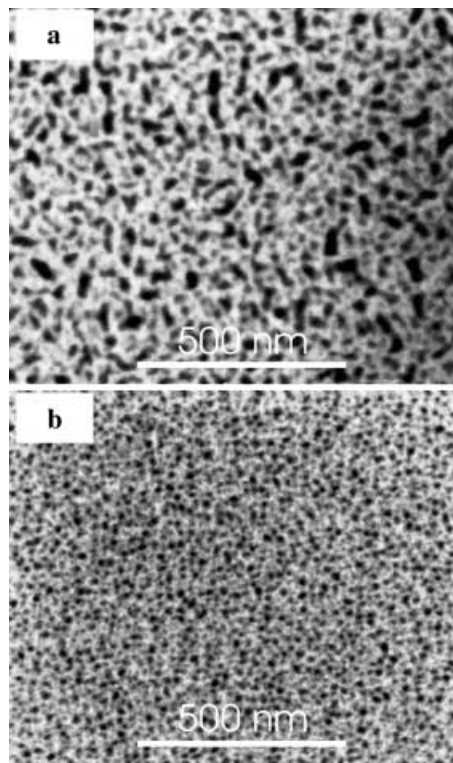

Fig. 2a,b. SEM plane-view micrographs of single layer PSi films formed by dc **a** and pulsed current **b** etching. Etching parameters used in **a** and **b** are those for the low refractive layer of the DBR, with effective etching time kept the same

sample (b) is more uniform and flatter than that of sample (a) formed by dc etching. A more uniform distribution of homogeneous pores and weaker lateral etching can be observed in image (b) than in image (a). In addition, although the two images were taken from the samples formed with the same current density and equivalent etching time, the pore size of PSi in image (a) is obviously larger than that in image (b), indicating a more effective control of the porosity using pulsed current etching than when using dc etching. This can be ascribed to the stronger lateral etching during dc etching than that during pulsed current etching and hence the smaller depth of pore (or film thickness) in the dc case. It is well known that the formation of the PSi layer is a self-limited process [10, 12, 13]. The chemical reaction of HF with Si will lead to the reduction of HF concentration inside the pore and thus decelerate the etching process itself. Furthermore, the species produced in the etching process will form bubbles on the wall surfaces of pores, which in turn prevent the progress of the etching process [8]. However, if the continuous dc etching is changed to an intermittent mode of pulsed current etching, it is expected that desorption of the bubbles and interchange of the HF species between the inside and outside of the pores will occur during the periodic pauses of anodic current. Therefore, the pulsed current mode could keep the anodic etching process operating in a more uniform way and thus produce a more homogeneous film than the dc mode, as is evident in images (b) and (a). In addition, when viewed by the naked eye, the PSi film prepared by pulsed current etching shines a uniform interference color in the sample area, while the interference color varies from the center to

the edge of the dc-etched sample. Comparison between the SEM plane-view images of the high refractive index or active layers formed by dc and pulsed current etching can lead to the same conclusions. That is to say, for the various current densities adopted, ranging from 6.7 mA/cm^2 to 83 mA/cm^2, the single layer PSi layers formed by pulsed current etching are always more uniform than those formed by conventional dc etching.

2.2 Cross-section of DBR and PSM

Figure 3 shows SEM cross-section micrographs of (a) a DBR, (b) a PSM, and (c) an active layer of the PSM. The fabrication process and parameters adopted for etching the reflectors and PSMs have been described in Sect. 1. From image (a) in Fig. 3, one can see that very flat interfaces, within the visible wavelength dimension, can be obtained by pulsed etching. Moreover, considering the deviation of the view angle and the existence of various cleavage-induced surface cracks, it is evident that good control and high reproducibility has been achieved for the pair thickness of the Bragg reflectors (except for the first pair). This is obviously important for the fabrication of the PSM structure. The first pair of upper Bragg reflectors is a little bit thinner than the pairs below. This is due probably to excessive chemical dissolution of PSi because of its relatively long residence in the electrolyte. From image (b) in Fig. 3, the sandwich structure in the PSM can be clearly distinguished, i.e. the active layer is enclosed between the two
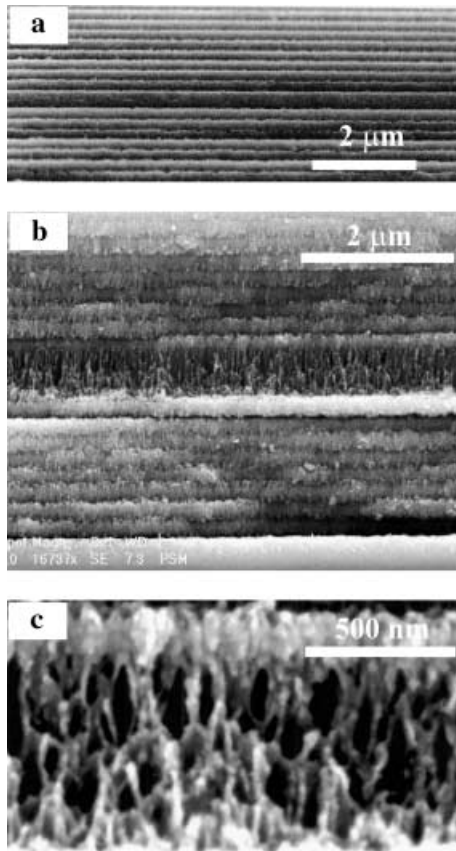
distributed porous silicon Bragg reflectors. It is also worth noting that use of the present pulsed current etching technique enables us to clearly observe the oriented 10-nm-scale Si columns along the etching direction within the active layer of the PSM (image (c)). To the best of our knowledge, such clear observation of the fine structure has not been reported in the literature for an active layer formed by conventional dc etching. Our technique may thus be used as an effective way to fabricate arrays of nanometer-diametric Si columns with high luminescent efficiencies at room temperature. The high film uniformity and interface flatness will bring good optical features to a PSM, too, as will be shown by the PL spectra in the section to follow.

Recent studies [14, 15] have shown that the difference in refractive index (porosity) of PSi formed from p^- (resistivity 0.1–0.5 Ωcm) or p (6 ~ 9 Ωcm) type Si substrates is small within a large range of current densities in comparison with that formed from p^+-type Si substrate, indicating that PSMs are harder to fabricate from lightly-doped Si substrates [15–17] with the dc technique. For these p^- or p-type Si substrates, related research work employing pulsed current etching is in progress.

3 PL spectra

3.1 Angular dependence

Angle-integrated PL spectra from the active layer PSi and the PSM are shown by curves (a) and (b) in Fig. 4, respectively. The spectra were excited by the 441.6 nm line of a He−Cd
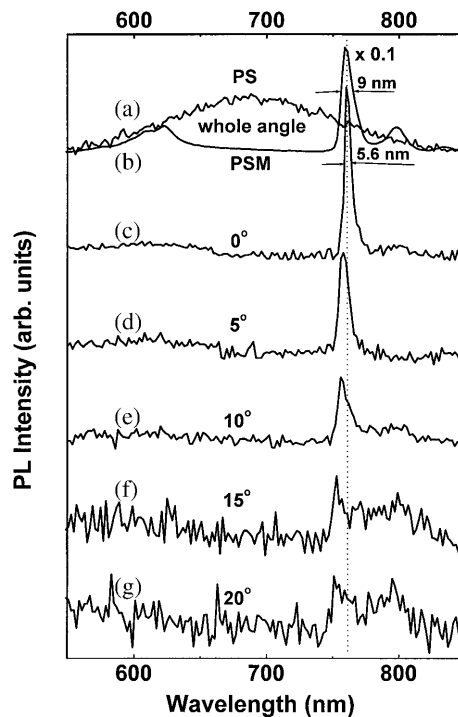

Fig. 3a–c. SEM cross-section micrographs of **a** a DBR, **b** a PSM, and **c** the active layer of the PSM. The fabrication process and parameters adopted for etching the reflectors and PSMs are described in the text

Fig. 4. Angle-integrated (a and b) and angle-resolved (c–g) PL spectra. Curves (a) and (b) are measured from active layer PSi and a PSM, respectively, and curves (c)–(g) are from the same PSM, with the emission angle deviating from the normal of the PSM surface by 0°, 5°, 10°, 15° and 20° in sequence

laser. The spot size on the sample was about 1 mm, with a power of 30 mW. Compared with the quite broad peak (about 150 nm in FWHM) in (a), the peak of the PSi in curve (b) is much narrower (about 9 nm in FWHM). In addition, the emission intensity has been enhanced by about one order of magnitude upon employing the sandwich PSM structure. However, beside the resonant peak of the PSM, the weak side peaks, originating from the two distributed Bragg reflector mirrors [11], can also be observed. Curves (c), (d), (e), (f) and (g) in Fig. 4 are the angle-resolved PL spectra of the PSM structure, corresponding to 0°, 5°, 10°, 15° and 20° deviation from the normal of the PSM surface, respectively. It has also been found in our experiment that the PL emission of PSMs shows an almost symmetric distribution around the normal of the sample surface. These angle-resolved PL spectra are characterized by the following distinct features: No shoulder peaks surrounding the resonant peak have been observed. Little PL signal emits from the PSM when the angle is larger than 10°, which means the narrowed resonant emission is highly directional and concentrated in a sharp cone normal to the PSM surface. In contrast, a 30°-divergence was previously reported in the literature [2, 6] for PL emitting from similar samples. Moreover, the peak measured in the angle-resolved mode further narrows from 9 nm to 5.6 nm in our case. It is thus established that spatially- and energetically-narrowed single-mode PL emission can be achieved from a PSM fabricated by the present pulsed current etching technique. This is due to the formation of both better interfaces between the layers of the two DBRs and oriented nanometer Si columns along the etching direction within the active layer, as illustrated by the SEM image of the cross-section of the PSM in Fig. 3.

Note that the present technique is actually applicable to the fabrication of PSMs centered at various wavelengths. Very recently, Lu et al. in this lab have successfully narrowed light emission from tri-(8-hydroxyquinoline) aluminum (Alq$_3$) at 500 nm and 4-(dicyanomethylene)-2-methyl-6-(p-dimethylaminostyryl)-4H-pyran (DCM)-doped Alq$_3$ at 660 nm by using the organic materials as active media in PSMs prepared by the pulsed current etching technique [18].

3.2 Aging effects

The effect of laser illumination on the PL of the PSM is shown in the top panel of Fig. 5, following exposure of the freshly prepared sample to the 441.6 nm laser beam. Curves (a), (b), (c), (d) and (e) correspond to an illumination time of 0, 3, 6, 9 and 12 min, respectively. The test dot on the PSM surface was marked so that further experiments to detect aging effects (shown in the bottom panel of Fig. 5) could be performed at the same place two weeks later. One may see from the top panel that, upon exposure of the freshly prepared PSM to the laser beam, the resonant peak of the PL was hardly influenced: the spectral intensity and line shape, especially the peak wavelength and the FWHM, remained nearly constant during the experiment. This indicates that the resonant peak of the PSM is quite stable under laser exposure. In contrast, the shoulder peaks show a slow decrease with the laser exposure time and stabilize after illumination for about 12 min.
The changes in the PL intensity and line shape versus exposure to a He−Cd laser for a typical P$^+$ PSM stored in air over
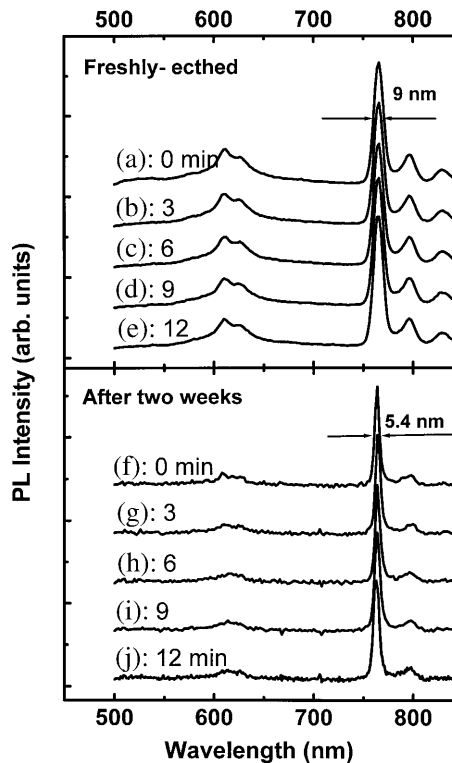

Fig. 5. PL from the PSMs upon exposure to the 441.6 nm laser beam. Top panel: the freshly prepared PSM. Bottom panel: the PSM stored over a period of two weeks. The figures noted on left of the curves are exposure time

a period of two weeks are shown in the bottom panel of Fig. 5. It is worth noting that the FWHM of the resonant peak becomes narrower (from 9 nm to 5.4 nm) and its intensity with respect to background emission becomes higher. Moreover, the position of the resonant peak remains nearly fixed. These results indicate that, during storage of the PSM sample in the relatively short period of two weeks, spontaneous oxidation mainly affected the top mirror, while the active layer and M$_2$ were hardly influenced. This is not so surprising because the outermost layers are likely to be oxidized prior to other layers. Therefore the top mirror oxidizes first in the sandwich structure of the PSM. Such homogeneous oxidation of the top mirror may improve the optical properties of the microcavity to some extent, as the difference in the refractive indices increases with increasing oxidation. This leads to a reduced peak width and enhanced intensity ratio of the peak to background emission. As is confirmed in the case of a random-geometry PSM [10], progressive oxidation is important for maintaining the coherence between the multiple reflections at the various interfaces, which explains the relatively good performance of aged PSMs. Although we have not measured the PL spectra of the PSM stored for a longer time, referring to a previous report in the literature [13], a shift of only several nm can be expected for this kind of P$^+$-doped Si substrate after one year of aging.

3.3 Further narrowing

Much better PL characteristics, as shown in the bottom panel of Fig. 6, can be achieved when the etching parameters used to fabricate the PSM are carefully adjusted. The reflectiv-
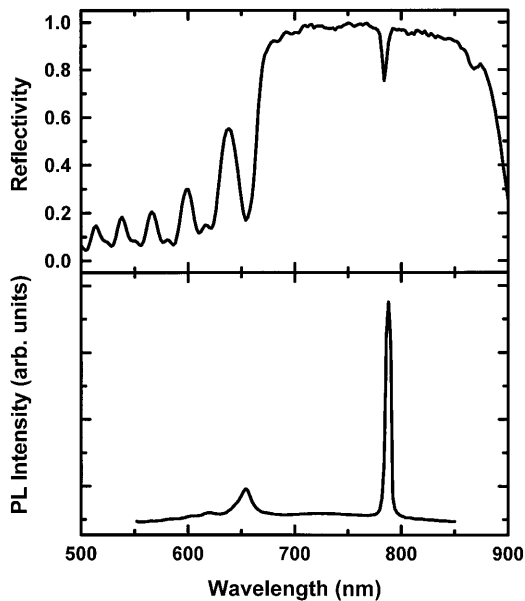
Fig. 6. Reflectivity (*top panel*) and PL emission (*bottom panel*) measured from a PSM fabricated by optimizing etching parameters such as current density and time

ity of the PSM is presented in the top panel. The reflectivity (relative to an Al mirror) is up to 99%, and the stopband is about 200 nm wide. The FWHM of the PL peak from the PSM is only 4 nm. To our knowledge, it is almost the narrowest FWHM of all the porous silicon microcavities composed of two periodically layered mirrors sandwiching an active layer ever reported (3.7 nm for a random-geometry PSM [10]). Moreover, the shoulder emission (leaky mode) is considerably weak compared to the resonant cavity mode, i.e. the ratio of signal to background is high. The enhanced PL emission from the PSM gives strong evidence that pulsed anodic etching, due to its orientation-selective penetration, can produce flatter interfaces in the DBR consisting of a PSM than conventional dc etching.

4 Summary

In conclusion, by employing a pulsed anodic etching technique in fabricating porous silicon microcavities, we have achieved a flat layered structure and improved PL emission. The single layer PSi formed by pulsed etching is more uniform and flatter than that formed by dc etching. There exist oriented

nanometer Si columns within the active layer, and good reproducibility and flat interfaces in the PSM and its two DBRs. The PL emission from the PSM exhibits highly directional (10° around the normal) and single-mode (without shoulders) features. Due to progressive oxidation of the top mirror, the refractive index difference between the high and low refractive layers increases with increasing storage time of the freshly prepared PSM in an ambient environment, which results in further narrowing of the PL peak. By optimizing etching parameters, a FWHM of 4 nm is achievable for the narrow PL peak from the freshly etched PSMs formed using the present technique. Better interfaces in the DBRs are regarded as a favorable factor for pulsed-current-etched PSM having good optical features.

References

1. L.T. Canham: Appl. Phys. Lett. **57**, 1046 (1990)
2. L. Pavesi, C. Mazzoleni, A. Tredicucci, V. Pallegrini: Appl. Phys. Lett. **67**, 3280 (1995)
3. V. Pellegrini, A. Tredicucci, C. Mazzoleni, L. Pavesi: Phys. Rev. B **52**, R14328 (1995)
4. M. Araki, H. Koyama, N. Koshida: Jpn. J. Appl. Phys. **35**, 1041 (1996)
5. Z.H. Xiong, S. Yuan, Z.M. Jiang, J. Qin, C.W. Pei, L.S. Liao, X.M. Ding, X.Y. Hou, Xun Wang: J. Lumin. **80**, 37 (1999)
6. S. Chan, P.M. Fauchet: Appl. Phys. Lett. **75**, 274 (1999)
7. X.Y. Hou, H.L. Fan, F.L. Zhang, M.R. Yu, X. Wang: In *Extended Abstracts of the 1995 International Conferences on Solid State Devices and Materials*, ed. by H. Ishiwara (The Japan Society of Applied Physics, Osaka, Japan 1995)
8. X.Y. Hou, H.L. Fan, F.L. Zhang, M.Q. Li, M.R. Yu, X. Wang: Appl. Phys. Lett. **68**, 2323 (1996)
9. Z.H. Xiong, S. Yuan, Z.M. Jiang, J. Qin, C.W. Pei, L.S. Liao, X.M. Ding, X.Y. Hou, X. Wang: J. Lumin. **80**, 137 (1999)
10. L. Pavesi, P. Dubos: Semicon. Sci. Technol. **12**, 570 (1997)
11. L. Pavesi, C. Mazzoleni, A. Tredicucci, V. Pellegrini: Appl. Phys. Lett. **67**, 3280 (1995)
12. M. Cazzanelli, L. Pavesi: Phys. Rev. B **56**, 15246 (1997)
13. C. Mazzoleni, L. Pavesi: Appl. Phys. Lett. **67**, 2983 (1995)
14. S. Frohnhoff, M.G. Berger, M. Thönissen, C. Dieker, L. Vescan, H. Münder, H. Lüth: Thin Solid Films **255**, 59 (1995)
15. V. Mulloni, C. Mazzoleni, L. Pavesi: Semicond. Sci. Technol. **14**, 1052 (1999)
16. S. Setzu, S. Létant, P. Solsona, R. Romestain, J.C. Vial: J. Lumin. **80**, 129 (1999)
17. M. Takahashi, Y. Toriumi, T. Matsumoto, Y. Masumoto, N. Koshida: Appl. Phys. Lett. **76**, 1990 (2000)
18. M. Lu, S.H. Xu, S.T. Zhang, J. He, Z.H. Xiong, Z.B. Deng, X.M. Ding: Acta Physica Sinica **49**, 2083 (2000) (in Chinese)